AIAA SciTech Forum
8-12 January 2024, Orlando, FL
AIAA SCITECH 2024 Forum

10.2514/6.2024-0849

Root Boundary Conditions for Omega Deployable Booms

Flavia Palmeri*
California Institute of Technology, Pasadena, California, 91125
Sapienza University of Rome, Rome, Italy, 00138

Susanna Laurenzi†
Sapienza University of Rome, Rome, Italy, 00138

Sergio Pellegrino‡
California Institute of Technology, Pasadena, California, 91125

We investigate how different root boundary conditions for Omega booms affect the two primary requirements: small stowed volume along with high bending stiffness in the deployed configuration. For each boundary condition two finite element models are developed using the Abaqus software. The first model simulates the coiling process and is intended to get insights into the mechanics of coiling and to retrieve the shape of the transition region between the boom coiled and extended configuration which is used in the second model for computation of the bending stiffness. A specific boom design has been chosen and a physical prototype has been built.

I. Introduction

Carbon fiber reinforced plastic (CFRP) booms are widely used deployable structures. Tubular deployable booms can be categorized according to the cross-section geometry into: Storable Tubular Extendible Member (STEM), Triangular Rollable and Collapsible (TRAC), SHEARLESS booms and Collapsible Tube Masts (CTM) or Omega booms. The STEM is a thin-walled composite shell with circular cross-section [1]. The TRAC boom is composed of two curved C-shaped section joined along one edge [2]. The SHEARLESS boom is formed by coupling the edges of two cylindrical shells front-to-front by a tightly-fitted outer sheath [3]. The Omega boom is made by joining along the edges, two omega-shaped shells formed by three circular arc segments: a central one, defined by radius r_1 and subtended angle α_1, and two outer arcs, defined by radius r_2 and subtended angle α_2 [4], Fig.1. In this paper, we examine the Omega boom which is attractive for many small satellite space missions [5].

The packaging scheme, the mechanism that drives the deployment/retraction of a boom and locks it in the deployed configuration, and the way the boom latches are all important points in the design of a boom. Motorized deployment uses electric motors in combination with mechanical components and a central deployment unit, around which the boom is wrapped [6]. At the end of deployment, the deployment unit provides an interlocking base for the boom root. In this work, a motorized mechanism having a central deployment unit is considered to deploy an Omega boom.

In a motorized mechanism with a central deployment unit (hub) the boom interface is provided by the deployment unit itself. Hence, the performance of the deployed boom cannot be studied independently of the coiling process. The boom-hub interface provides the root boundary condition (BC) which must be carefully designed to allow compact, damage-free coiling while ensuring that the boom's operational performance is as intended. These two primary requirements - a small stowed volume along with a high bending stiffness and strength - are in competition. On one hand, a cantilevered boom with a flattened and clamped root BC can be easily wrapped around a very small hub for compact stowage, but it also requires a long gradual shape transition for its cross section to flatten. This region has a much reduced load bearing capability. On the other hand, a boom with a clamped-root BC at the boom-deployment unit interface has no local weakening but will likely suffer excessive material strain, leading to buckling and potential damage when it is coiled.

Previous studies have proposed several strategies, featuring different boundary conditions (BCs). Some aim at mitigating

*Visiting researcher, Graduate Aerospace Laboratories, MC 105-50. PhD Student, Department of Mechanical And Aerospace Engineering. Corresponding author. E-mail: flavia.palmeri@uniroma1.it.

†Full Professor, Department of Astronautical Electrical and Energy Engineering, E-mail: susanna.laurenzi@uniroma1.it.

‡Joyce and Kent Kresa Professor of Aerospace and Civil Engineering; Jet Propulsion Laboratory Senior Research Scientist; Co-Director, Space-Based Solar Power Project, Graduate Aerospace Laboratories, MC 105-50. AIAA Fellow. E-mail: sergiop@caltech.edu.

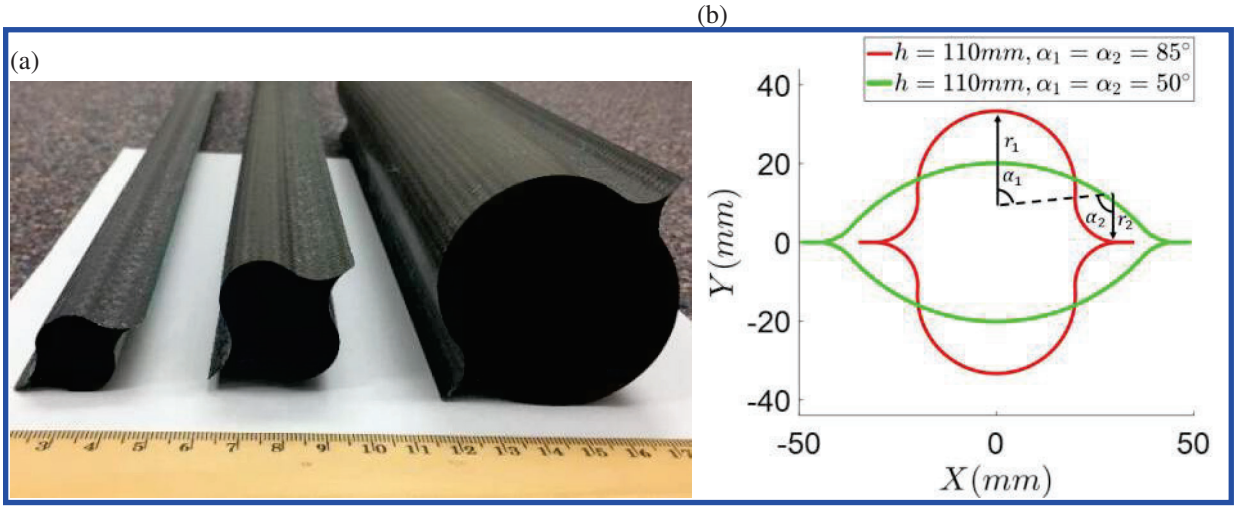

Fig. 1 a) Thin-shell Omega composite booms developed at LaRC with flattened widths of h=45 mm, 65 mm, and 110 mm, Image courtesy of NASA. b) Cross-sections of Omega booms, flattened width h=110 mm and subtended angles of $\alpha_1 = \alpha_2 = 85°$ (red line) and $\alpha_1 = \alpha_2 = 50°$ (green line). Each shell is formed by three circular arc segments: a central arc defined by a radius r_1 and subtended angle α_1, along with two edge arcs defined by a radius r_2 and subtended angle α_2

.

the performance reduction at the transition region while others allow for compact coiling even if the boom develops its full root section within the deployment mechanism. Different ways of counteracting the mechanical performance reduction have been proposed. In Ref.[7] truss-like structures were placed adjacent to the central hub, forming an outer collar shaped like the opening boom. Ref.[8] designed an outer support shell and a floating inner core held in place by localized elastic deformation of the boom. Two different strategies have been proposed to lower the strain of the laminate coiled around a small hub with the boom full section clamped. In Ref.[9] the CFRP boom region adjacent to the root area is replaced with a metallic shell forming a hinge capable of withstanding a small curvature radius. In Refs. [10]-[11] the root cross-section of a boom is expanded by an additional mechanism.

In this paper, a novel interface is presented for connecting an Omega boom to its deployment mechanism, aiming at shortening the transition while mitigating excessive strain in the CFRP laminate. This interface features a partially clamped root BC, i.e. a BC which constrains all the degrees of freedom of an open root cross-section, after removal of some material of the boom to reduce the maximum strains induced by folding.

Two numerical simulations are conducted to obtain an understanding of how the novel interface behaves. A coiling simulations is run to assess whether this new interface enables a short transition region while avoiding excessive stress concentration while a second simulation estimates the bending stiffness of the deployed boom.

To study the effectiveness of the proposed strategy, the results of these simulations are compared with case studies inspired by the interfaces developed in Refs. [7]-[10].

Section II presents the partially clamped root BC concept. Section III provides an overview of all the case studies that are analyzed and compared. In Section IV the finite element models are described. The coiling and bending stiffness simulations are presented in Section V and Section VI, respectively. In Section VII the simulations results are shown and discussed. In Section IX an experimental demonstration of the partially clamped root cross-section is presented. Section X concludes the paper.

II. Partially clamped root concept

In the partially clamped root cross-section, all of the degrees of freedom of an open root cross section are constrained but not the full closed cross-section.

The concept involves removing material from the boom near the clamped root to create a structure that is able to fold with a small radius of curvature while avoiding curvature localization [12]. To do so, the bonding region between the

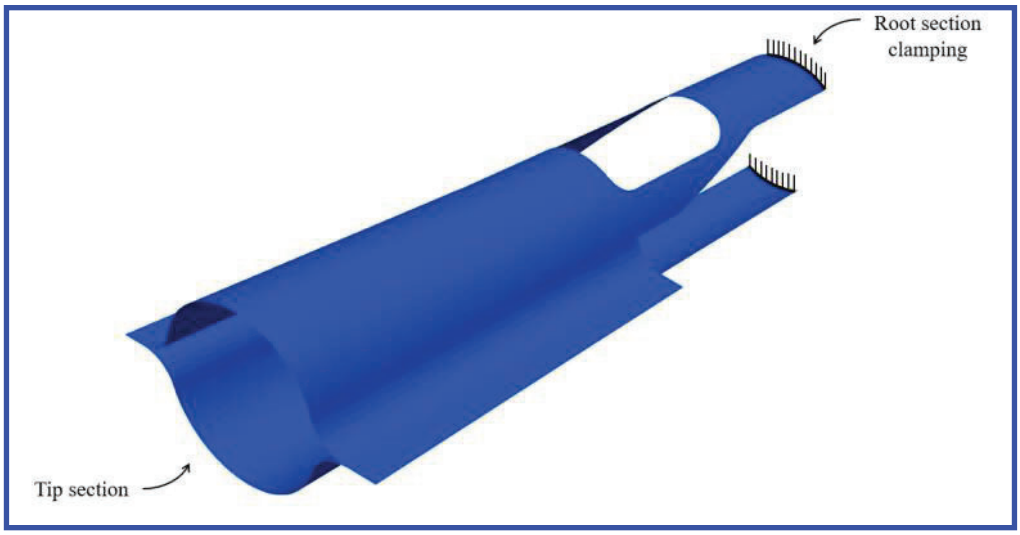

Fig. 2 Partially clamped root cross-section BC concept.

two shells is completely removed as well as the edge arc segments. Additional material is removed from the central arc segment of both top and bottom shells. The idea is that the leftover material forms two tape springs. The top tape spring has a central hole that allows the bottom tape spring to fold within it. This design, shown in Fig.2, enables the bottom half to fit into the hole of the top half after folding. The shape was designed through a trial-and-error process utilizing finite element analysis, aiming to minimize the maximum stresses in the stowed configuration.

III. Boundary conditions under study

In this work we investigate how four different BCs affect the compactness of stowing and the structural performance under bending. The BCs under study are derived from the partially clamped root BC concept and from some strategies presented in the literature [7]-[10]. The cases under study are the following:

Flattened and clamped root BC with outer shell. The boom is cantilevered with its root cross-section clamped to the external surface of a cylindrical hub, after being flattened. An outer shell in added in correspondence of the transition zone.

Flattened and clamped root BC with outer shell and inner core. The boom is cantilevered with its root cross-section clamped to the external surface of a cylindrical hub, after being flattened. An inner core is added along with an outer shell in correspondence of the transition zone.

Partially clamped root BC. The boom is cantilevered with part of its root cross-section clamped to a planar surface within the cylindrical hub. This planar surface was obtained by removing a quarter of the cylinder from the hub.

Fully clamped root BC. The boom is cantilevered with its full root cross-section clamped to a planar surface within the cylindrical hub. This planar surface was obtained by removing a quarter of the cylinder from the hub.

The BCs under study are shown schematically in Fig.3. The flattened and clamped root BC with the outer shell, the flattened and clamped root BC with the outer shell and inner core, the partially clamped and the fully clamped root BC are shown in Fig.3a, Fig.3b, Fig.3c and Fig.3d, respectively.

IV. Finite element models

Finite element models are developed to study the behavior of an Omega boom with the four different root BCs described in Section III using the commercial finite element software Abaqus, 2020 [13].

Each model consists of two main parts: a rigid coiling hub and an Omega boom.

The boom length is $l = 1$ m. The geometry of the boom cross-section is provided in Fig.4, where $r_1 = 25.00$ mm is the radius of the central arc segment, $r_2 = 11.00$ mm is the radius of the edge arc segment, $x_{0,1} = 0.0$ mm $y_{0,1} = 1.68$ mm describe the origin of the central arc segment, $x_{0,2} = 24.15$ mm and $y_{0,2} = 11.0$ mm indicate the origin of the edge arc segment, and $x_1 = 24.15$ mm, $x_2 = 34.65$ mm, $x_3 = 42.65$ mm are the positions along the x-axis of the points furthest from the y-axis of the central arc segment, of the edge arc segment and of the web, respectively.

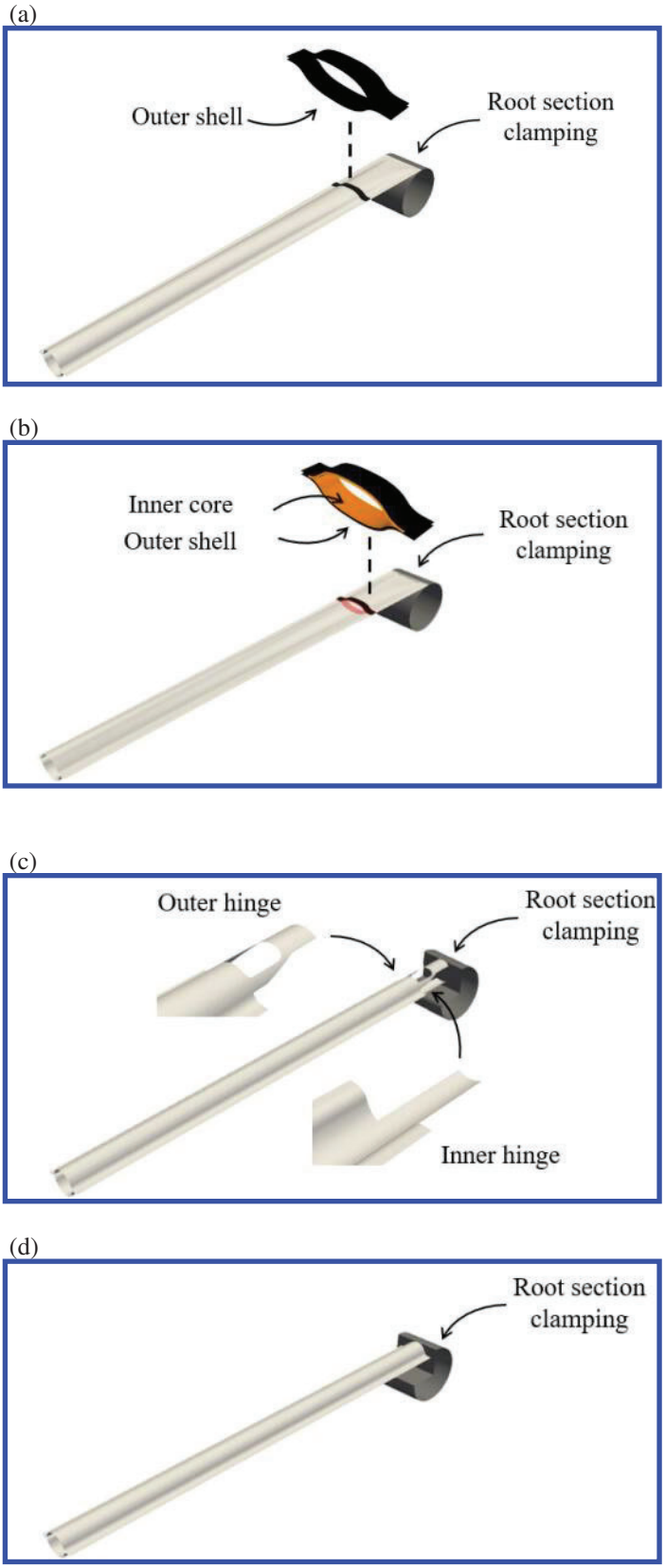

Fig. 3 Comparison of root BCs: (a) flattened and clamped root BC with outer shell and lateral support, (b) flattened and clamped root BC with outer shell, inner core and lateral support, (c) partially clamped root BC, (d) fully clamped root BC.

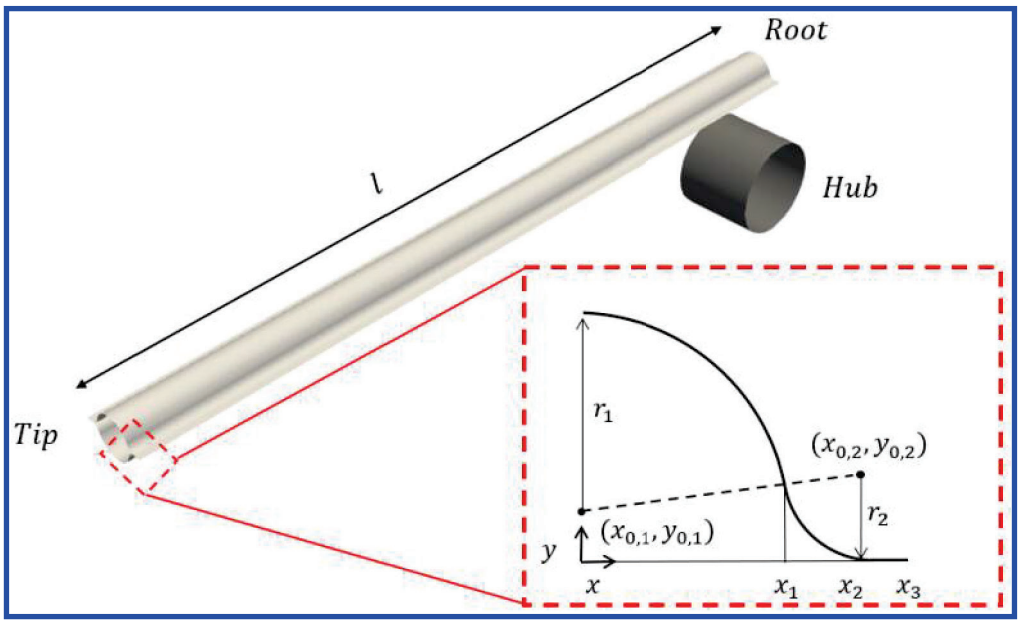

Fig. 4 Geometric description of the Omega boom: r_1, $x_{0,1}$ and $y_{0,1}$ are the radius and origin coordinates of the central arc-segment, r_2, $x_{0,2}$ and $y_{0,1}$ are the radius and origin coordinates of the edge arc-segment and the x_1, x_2 and x_3 are the x coordinates of respectively the central arc-segment, the edge arc-segment and the web ends.

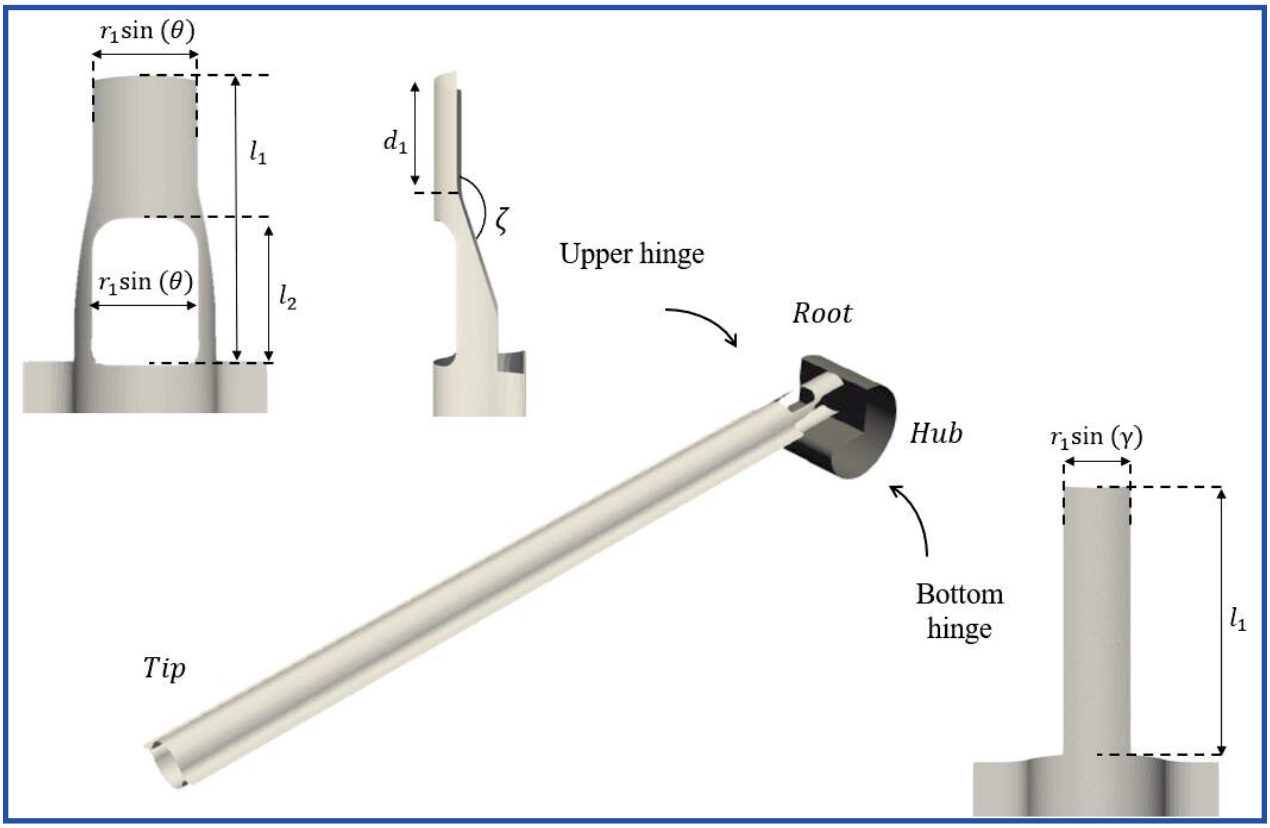

Fig. 5 Detailed description of the partially clamped root cross-section BC: θ and l_1 are respectively the width and length of the cylindrical strip in the top shell, θ and l_2 are the width and length of the hole in the cylindrical top strip, ζ and l_2 are respectively the broadening angle and its starting point, γ and l_1 are the width and length of the cylindrical strip in the bottom shell.

In the case of the partially clamped root BC, the slots geometry is defined in Fig.5. The parameters defining the cylindrical strip in the top shell are: the width and the length of the strip, $\theta = 45°$ and $l_1 = 100$ mm, respectively; the width and the length of the hole, $\theta = 45°$ and $l_2 = 50$ mm, respectively; the broadening angle, $\zeta = 165°$, and the position, $d_1 = 50$ mm, at which tapering begins. The parameters defining the cylindrical strip in the bottom shell are the width and the length of the strip, $\gamma = 30°$ and $l_1 = 100$ mm.
To allow the Omega booms with partially and fully clamped root BC to fit into the volume previously occupied by the removed quarter of the hub, the hub radius is chosen as $R_{Hub} = 70$ mm and this value is kept equal for all the four cases considered.
The boom is made of isotropic material with Young's modulus $E = 70$ GPa, Poisson's ratio $\nu = 0.2$ and thickness $t = 72$ μm. The finite element mesh consists of 4-node reduced integration Reissner–Mindlin thin shell elements, S4R. The finite element models are intended to simulate the coiling mechanics and to estimate the bending stiffness for each BC. The two simulations are not independent. For the flattened and clamped root Bcs, Fig.3a-b, the coiling simulation not only elucidates its mechanism but also gives the shape of the transition zone between the fully fattened and the fully opened configuration. The transition zone shape is used for the subsequent computation of the bending stiffness of the deployed boom. For the case in which the root is partially clamped, Fig.3c, the the coiling simulation plays a crucial role in validating the adequacy of the slot design giving eventually its final shape, i.e. through the coiling we were able to scrutinize and refine the slot design until a suitable configuration was achieved.

V. Coiling simulation

This section presents a simulation of coiling for BCs involving flattening and clamping the root and also a simulation of coiling for the a boom with partially clamped root BC. A single coiling simulation was run for the case of a flattened and clamped root BC, both in the case of reinforcement with only an outer shell and in the case of an additional support with both an outer shell and an inner core, as the rolling mechanism remains unaffected by the addition of external supports introduced downstream.
The entire coiling process was simulated to verify that folding of the boom is possible, with the changes of curvature being less than 200 1/m.
In Ref.[14], buckle formation during coiling was found to lead to almost double the bending stresses that are predicted using a basic analysis that neglects buckling. Not to lose information on the local stress increase due to the buckle formation, in the present work the formation and propagation of buckle is accounted for.
A material-oriented coordinate system, aligned with the longitudinal and transverse coordinates of the boom, was established for the shell elements. The local axes, denoted as 1, 2, and 3, correspond to the longitudinal, transverse, and normal directions of the shell, respectively. Form the variation of curvature tensor in the local material frame, we derived its invariant and principal value:

$$\Delta\bar{K} = \frac{\Delta K_1 + \Delta K_2}{2} \tag{1}$$

$$\Delta K_{min} = \frac{1}{2}(2\Delta\bar{K} - \sqrt{4\Delta K_{12}^2 + (\Delta K_1 - \Delta K_2)^2}) \tag{2}$$

$$\Delta K_{max} = \frac{1}{2}(2\Delta\bar{K} + \sqrt{4\Delta K_{12}^2 + (\Delta K_1 - \Delta K_2)^2}) \tag{3}$$

The changes of principal curvature are then compared to the maximum allowable value to assess if the coiling process is damage free.

A. Coiling simulation, flattened and clamped BCs

A numerical simulation of the coiling process for a boom with flattened and clamped root BCs is run to get insight into the coiling mechanics and to determine the shape of the transition zone which is needed for the following simulation. For a boom with flattened and clamped root BCs, the coiling simulation consists of two quasi-static time steps carried out with the Dynamic-Implicit module in Abaqus.
In the first simulation step, the boom is flattened by applying two transverse tensions F along the edges of the webs, close to the root. Then, the rigid hub is moved towards the boom while a pressure is applied over the clamped area of the top shell, Fig.6. In the second step, an axial force is applied to the ends of the web, at the tip section, to ensure

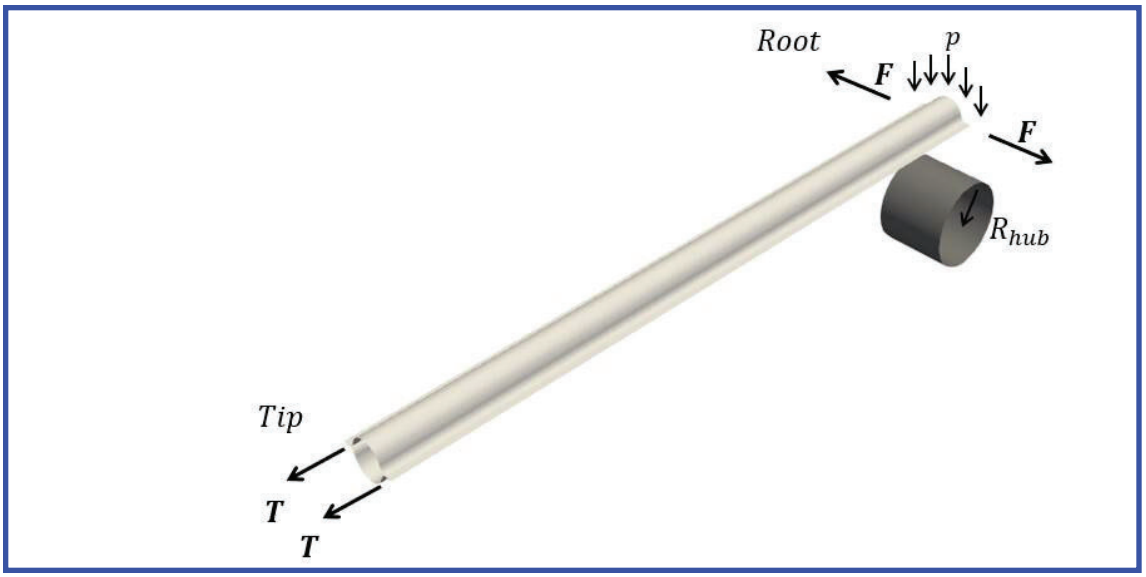

Fig. 6 Finite element model of coiling simulation for flattened and clamped root BCs.

compact coiling. The final step simulates coiling by rotating the hub and creating a rough contact area between the hub and the clamped root, which prevents any sideways movements, thus ensuring successful reeling onto the hub.

B. Coiling simulation, partially clamped BC

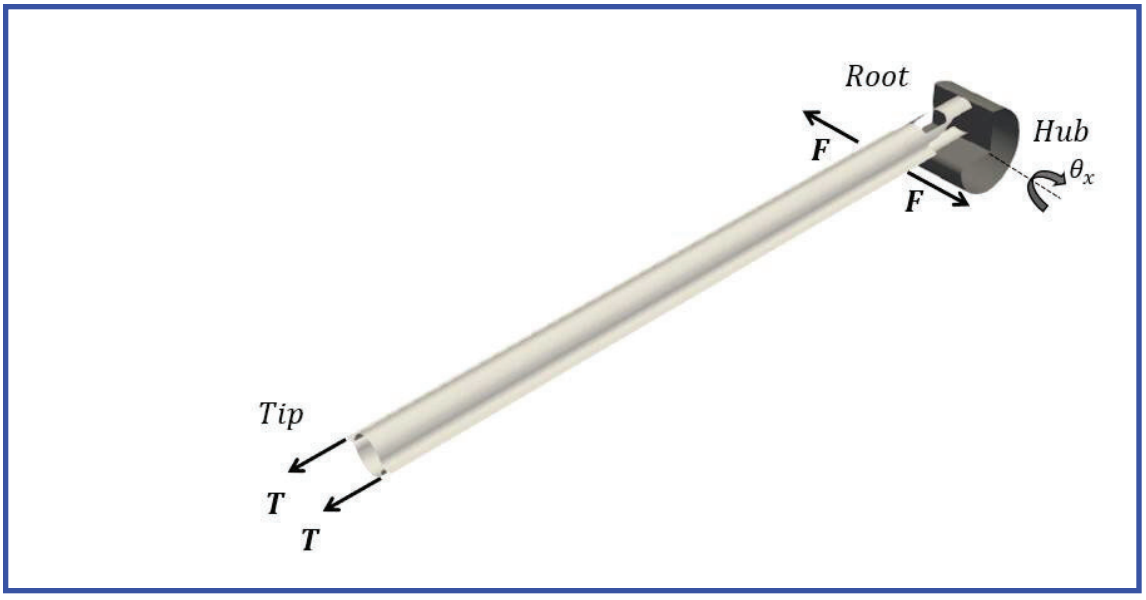

Fig. 7 Finite element model of coiling simulation for the partially clamped root BC.

The numerical simulation of the coiling process of the boom with partially clamped root BC is performed to better understand its mechanics and to fine-tune the slot design .The model, shown in Fig.7, consists of the rigid coiling hub and the boom. The rigid hub has a radius of 70 mm and a quarter of the hub has been removed to accommodate the boom attachment. The top and bottom shell root cross-sections were connected with the hub by tie constraints.
For a partially clamped root BC, the coiling simulation consists of three different quasi-static time steps carried out with the Dynamic-Implicit module in Abaqus. In the first simulation step, the top and bottom shell root cross-sections are

connected with the hub by tie constraints and the flattening process is initiated by applying two transverse forces F along the edges of the webs in correspondence of the end of the cylindrical strip. In the second simulation step, a fold is created by rotating the hub through 90°. The final step simulates coiling by applying a pressure over the flattened area of the top shell, beyond the fold, and by creating a rough contact area between the corresponding area of the bottom shell and the hub. The hub is then rotated and a tension is applied at the tip of the web regions to ensure a compact coiling.

VI. Bending stiffness analysis

Four different models have been developed to compute the bending stiffness of the Omega booms with four different root BCs using the Abaqus software.

All of the models consist of the rigid hub and the elastic boom, whose shape is different depending on the specific BCs under investigation. For flattened and clamped root BCs, the actual shape is retrieved from the deformed boom at the beginning of the coiling simulation, while for the clamped root BCs, whether partially clamped or fully clamped, the boom is in its undeformed shape.

For flattened and clamped root BCs, the inner and outer support shells must conform to the geometry of the deformed boom at the interface location. The geometry of the boom core aligns with the internal shape of the boom's transition zone, while the external support shell matches the external shape at a distance from the root such that the boom has developed 50% of its full cross sectional height.

The simulation consists of a single static general step. The BCs were defined with Multi Point Constraints (MPCs). The edge points at the root cross-section have been associated with a reference point (RP) created at the center of the corresponding section. The root RP is constrained against x, y, z translation and x, y, z rotation, to simulate the attachment of the boom to the central hub. The edge points at the tip cross-section have been associated with a RP created at the center of the tip cross-section. The bending moment is applied to the tip RP during each analysis.

VII. Coiling simulation results

A. Coiling simulation, flattened and clamped BCs

The results of the coiling simulation when the root is flattened and clamped are presented here.

The principal changes of curvature at the end of the flattening step are shown in Fig.8. It can be seen that there are two areas corresponding to the outer arc-segments of the boom where humps or dimples have formed. The maximum curvature change remains below 200 1/m and we can assume that the no-damage condition is satisfied for the entire flattening process.

As the coiling process progresses, we observed buckles forming at each of the outer arc-segments of the bottom shell of the boom. These buckles gradually increase in size until they meet at the center of the central arc-segment of the bottom shell and coalesce in a single buckle. As the boom is rolled, new buckles form, grow in size and coalesce. This results in the repeating pattern of humps and dimples shown in Fig.9. The maximum magnitude of curvature change is 170 1/m, thus the no-damage condition is met.

B. Coiling simulation, partially clamped BC

The results of the coiling simulation in the case of partially clamped BC are presented here.

The principal changes of curvature at the end of the folding step are shown in Fig.10. The maximum magnitude of the curvature change is found in the top shell. Indeed, Fig.10b shows a localization with high curvature changes close to the clamped root, with a maximum value of 190 1/m. Because this value is lower than the upper limit of 200 1/m, the fold is damage-free.

In the subsequent coiling step, the formation of a buckle is seen at the bottom shell. The buckle gradually increases in size until it reaches the stable configuration shown in Fig.11. Then it travels along the shell as the boom is coiled, without any changes of shape. The localized changes of curvature caused by the buckle formation and propagation do not affect the safe coiling of the boom structure.

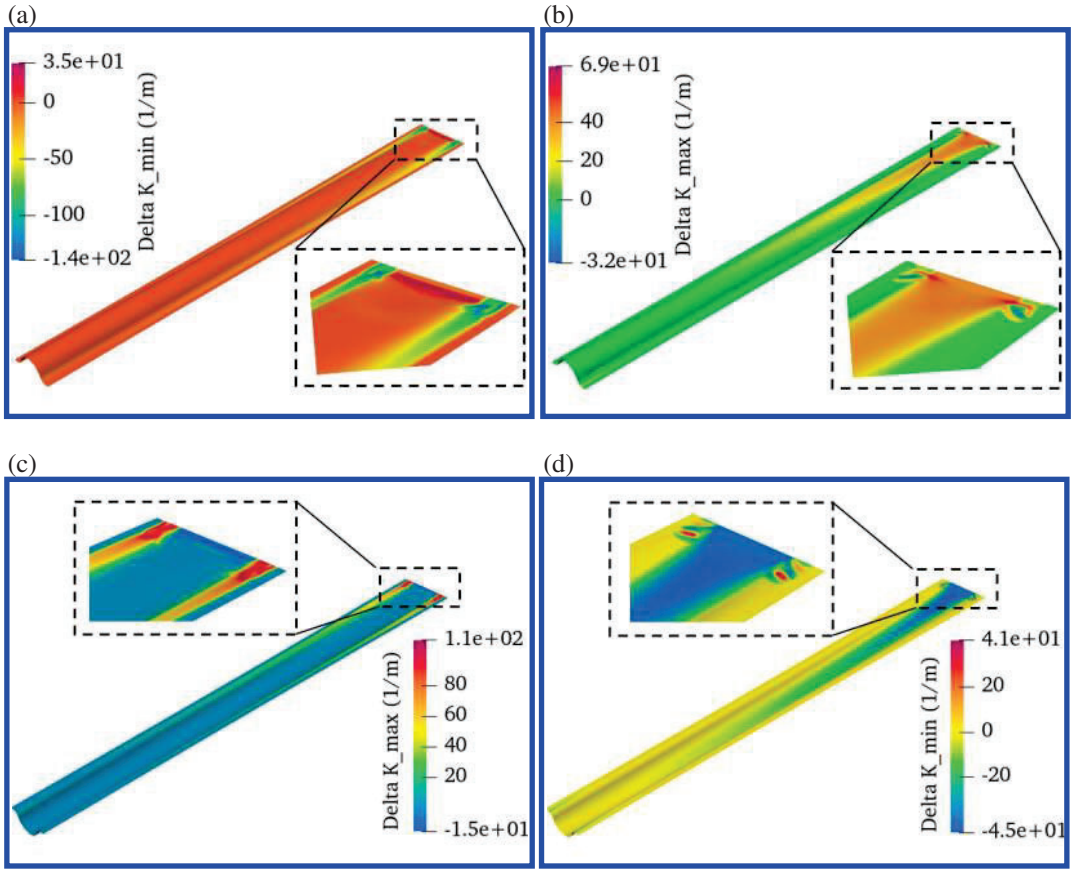

Fig. 8 Principal changes of curvature at the end of the flattening step for flattened and clamped BC: (a) change of maximum curvature in the top shell, (b) change of minimum curvature in the top shell, (c) change of maximum curvature in the bottom shell (d) change of minimum curvature in the bottom shell.

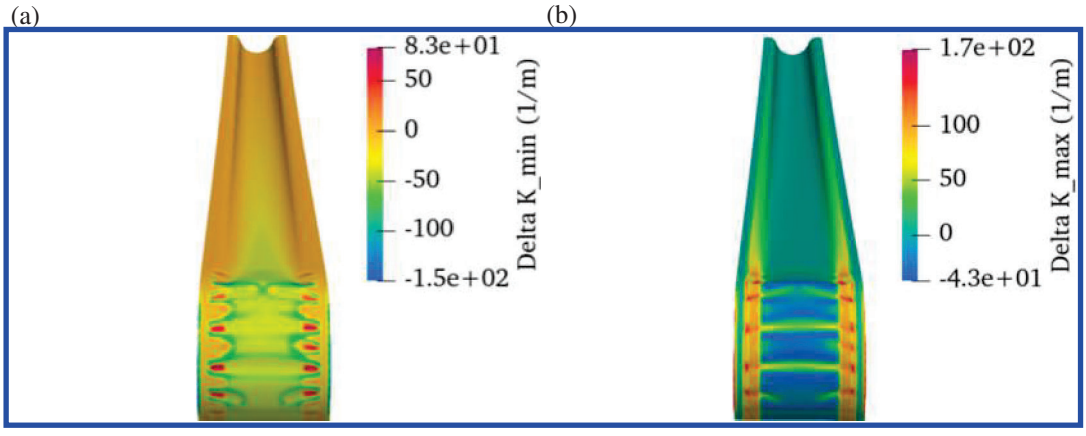

Fig. 9 Principal changes of curvature during the coiling step for flattened and clamped BC: (a) change of maximum curvature in the bottom shell , (b) change of minimum curvature in the bottom shell.

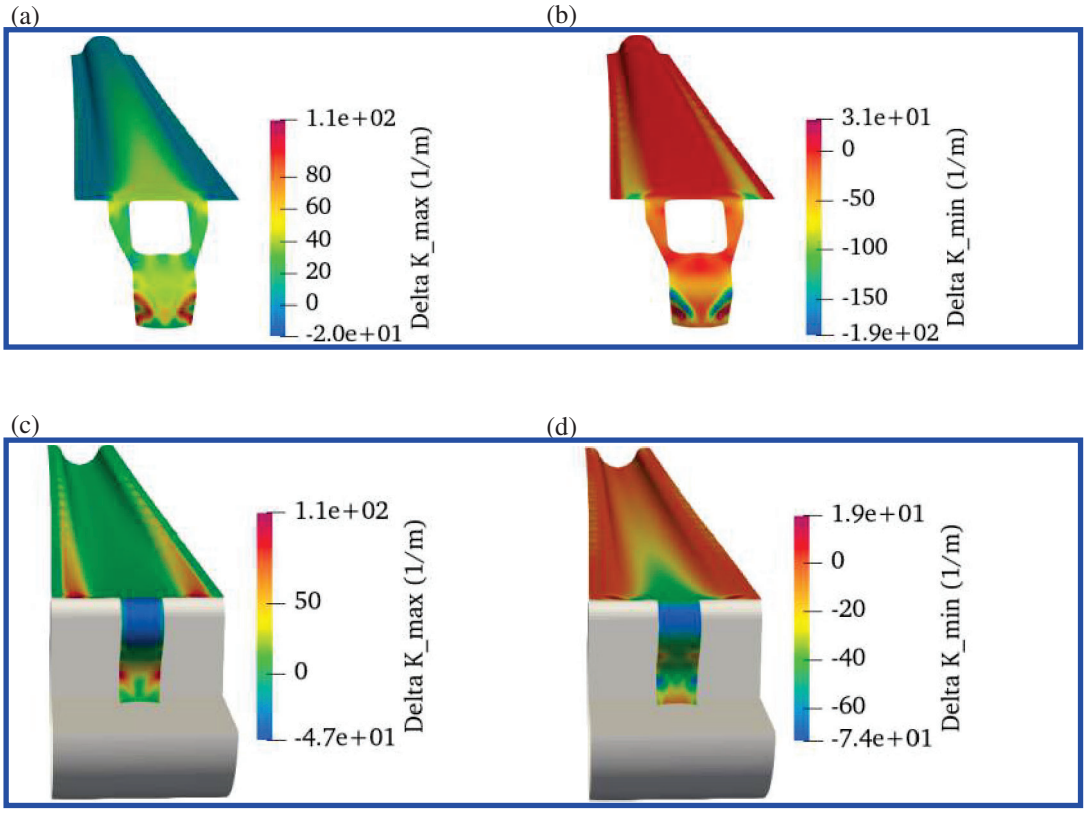

Fig. 10 Principal changes of curvature at the end of the folding step for the partially clamped root BC: (a) change of maximum curvature in the top shell, (b) change of minimum curvature in the top shell, (c) change of maximum curvature in the bottom shell (d) change of minimum curvature in the top bottom shell.

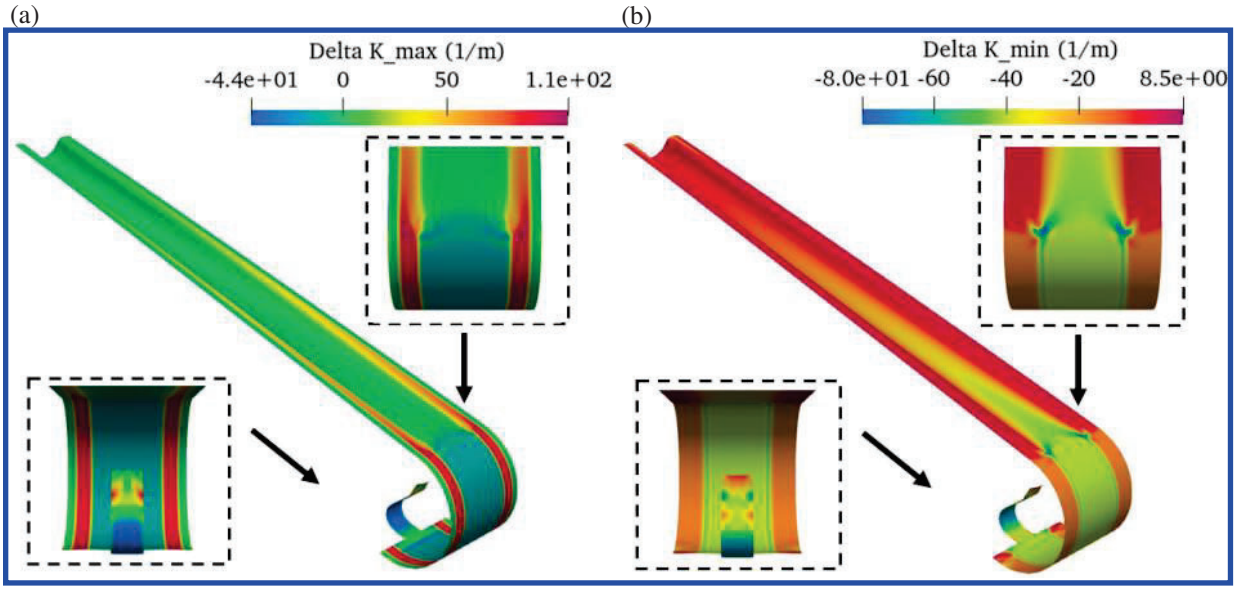

Fig. 11 Principal changes of curvature during steady state coiling for partially clamped root BC: (a) change of maximum curvature in the top bottom shell, (b) change of minimum curvature in the bottom shell.

Root BC	Tip deflection
Flattened and clamped, outer shell	7.36 mm
Flattened and clamped, outer shell and inner core	7.48 mm
Partially clamped	2.46 mm
Fully clamped	1.47 mm

Table 1 Tip deflection for different root BCs under unit bending moment applied to the tip.

VIII. Bending stiffness simulation results

For a unit bending moment, the tip deflections are summarized in Tab.1. The boom structure with fully clamped root BC has the highest bending stiffness as the tip deflects by only 1.47 mm. The boom with flattened and clamped root BC with just external support is the weakest in bending, its tip deflection being 7.48 mm which is 5.1 times larger than the fully clamped boom. Only a slight improvement is obtained by adding an inner core along with the outer supports, with the displacement of the tip being decreased by 24%. For the partially clamped root the tip deflection is 2.48 mm, which is almost 3 times lower compared to the flattened and clamped root BCs, either with or without the inner core, and only 1.7 times larger than the fully clamped boom .

IX. Prototyping

Prototypes of an Omega boom with a partially clamped root BC have been manufactured in an autoclave with a two-cure process. First, two bi-convex shaped shells were fabricated separately and bonded together in the following step. We used ultra-thin composite prepregs with the stacking sequence $[\pm 45_{GFPW}/\ 0_{CF}\ /\pm 45_{GFPW}]$, where GFPW denotes E-glass fabric (style 1067, 31 gsm) glass fiber plain weave prepreg and CF represents a unidirectional MR70 carbon fiber prepreg tape with North Thin Ply Technology 415 epoxy system (30 gsm). The total thickness of the resulting 3-ply laminate is approximately 70 µm .

Initially, the laminate was draped over male shaped aluminum molds to manufacture the shells. The top and bottom parts were vacuum-bagged and autoclave-cured. The shells were demolded and cut according to the slots design using a digital cutter.

Subsequently, the cured parts were placed on two female molds, having the negative shape of the male molds used for the first curing process. An additional ply of glass fiber plain weave, oriented at ±45° to the mold axis, was added in correspondence of the web regions on one of the shell. The molds were clamped together using bolts to apply a sufficient consolidation pressure to the web region. Tightening of the bolts ensured consistent consolidation throughout the structure. This resulted in a 7-ply web region with the stacking sequence $[\pm 45_{GFPW}/\ 0_{CF}\ /\pm 45_{3,GFPW}\ /0_{CF}\ /\pm 45_{GFPW}]$. A second autoclave process was then performed to cure the bonding ply.

A 30 cm long prototype is shown in Fig.12, both in its deployed and folded configurations.

X. Conclusions

This paper has described a new type of interface for Omega booms. The interface is based on a partially clamped root cross-section, which consists in constraining all the degrees of freedom of a portion of the full root cross-section. The design of the residual material underwent iterative refinement through finite element analysis simulations. The design herein presented involves creating tape springs through selective material removal, enabling compact folding while avoiding curvature localization. The effectiveness of this solution is observed during both the coiling process and in the deployed boom configuration. Coiling simulations demonstrate damage-free stowage around a central hub with a 70 mm radius. In the first coiling simulation step, which corresponds to a hub rotation through 90°, the highest curvature is experienced is in the top shell and it always remains below the damage-free threshold ensuring a safe folding. In the subsequent step, a buckle forms in the bottom shell while the boom is coiled. It gradually increasing in size until it stabilizes and travels along the shell. The buckle formation does not drastically affect the overall deformed boom shape and a damage-free coiling is still ensured. Additionally, competitive structural performance is observed in the bending stiffness analysis of an Omega boom which makes use of this new interface type. The tip displacement, when a unit bending moment is applied, is only 1.7 times larger than the minimum achievable by a boom with fully clamped root BC. Finally, a prototype has been manufactured which exhibits behavior consistent with simulation predictions.

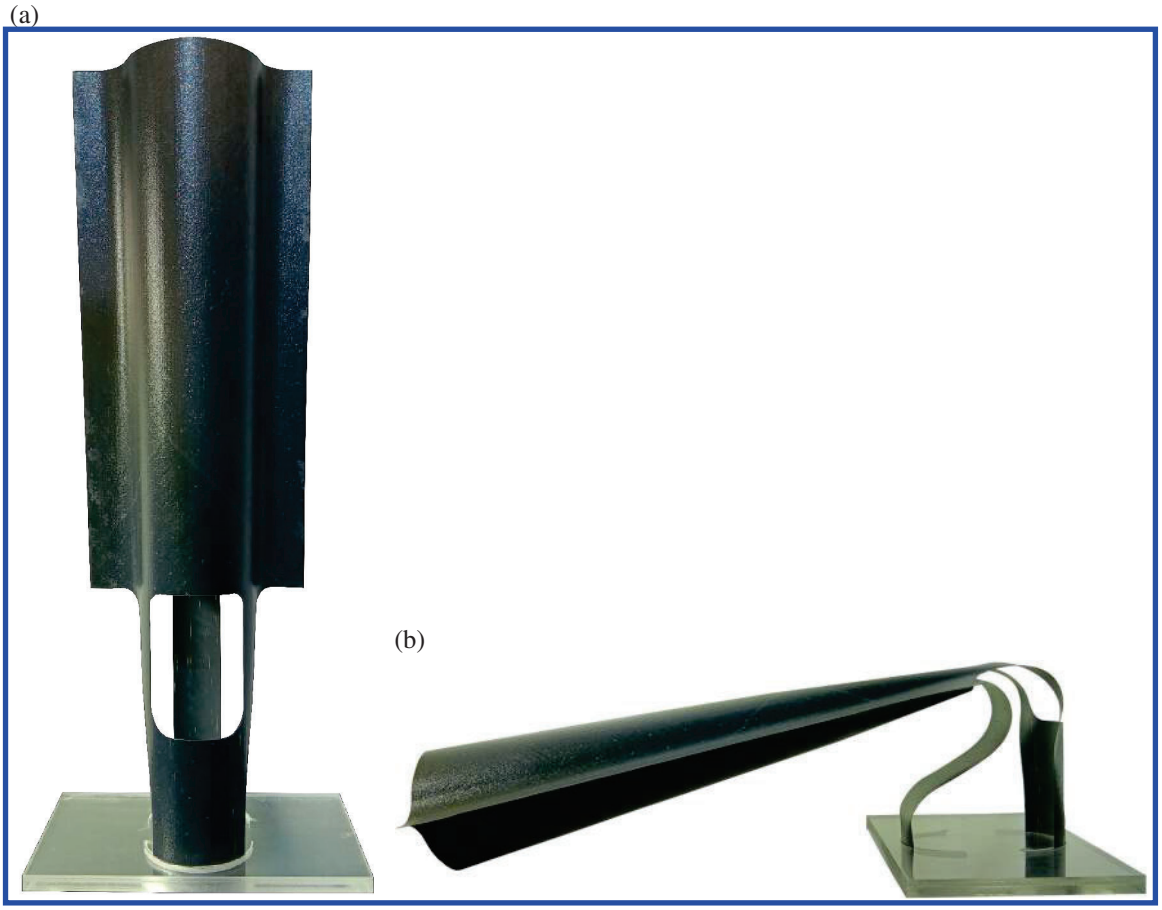

Fig. 12 Prototype of the partially clamped root BC: a) deployed configuration, b) folded configuration.

Acknowledgments

Financial support form the PhD programme in Aeronautical and Space Engineering at the University of Rome La Sapienza is appreciatively recognized.
Support from the Space Solar Power Project at Caltech, USA is gratefully acknowledged.

References

[1] Rimrott, F. P. J., "Storable tubular extendible member: a unique machine element," *Machine Design*, Vol. 37, No. 28, 1965, pp. 156–165.

[2] Leclerc, C., Wilson, L. L., Bessa, M. A., and Pellegrino, S., "Characterization of ultra-thin composite triangular rollable and collapsible booms," *4th AIAA Spacecraft Structures Conference*, 2017, p. 0172.

[3] Fernandez, J. M., "Sheath-based rollable lenticular-shaped and low-stiction composite boom," , Jan. 9 2018. US Patent 9,863,148.

[4] Stohlman, O. R., Zander, M. E., and Fernandez, J. M., "Characterization and modeling of large collapsible tubular mast booms," *AIAA Scitech 2021 Forum*, 2021, p. 0903.

[5] Fernandez, J. M., "Advanced deployable shell-based composite booms for small satellite structural applications including solar sails," *International Symposium on Solar Sailing*, 2017.

[6] Fernandez, J. M., Rose, G., Stohlman, O. R., Younger, C. J., Dean, G. D., Warren, J. E., Kang, J. H., Bryant, R. G., and Wilkie, K. W., "An advanced composites-based solar sail system for interplanetary small satellite missions," *2018 AIAA Spacecraft Structures Conference*, 2018, p. 1437.

[7] Sproewitz, T., Banik, U., Grundmann, J.-T., Haack, F., Hillebrandt, M., Martens, H., Meyer, S., Reershemius, S., Reininghaus, N., Sasaki, K., et al., "Concept for a Gossamer solar power array using thin-film photovoltaics," *CEAS Space Journal*, Vol. 12, 2020, pp. 125–135.

[8] Hillebrandt, M., Zander, M. E., and Huehne, C., "Sliding Core Deployment Mechanism for Solar Sails based on Tubular Shell Masts," *5th International Symposium on Solar Sailing*, Aachen, Germany, 2019.

[9] Okuizumi, N., Watanabe, A., and Ito, H., "Efficient Storage and Deployment of Tubular Composite Boom Using Spring Root Hinges," *Journal of Spacecraft and Rockets*, Vol. 58, No. 2, 2021, pp. 334–344.

[10] Straubel, M., and Hühne, C., "CTM Boom Deployment Mechanism with Integrated Boom Root Deployment for Increased Stiffness of the Boom-to-Spacecraft Interface," *European Conference on Spacecraft Structures, Materials and Environmental Testing (ECSSMET 2021)*, Berlin, Germany, 2021.

[11] Stabile, A., and Laurenzi, S., "Coiling dynamic analysis of thin-walled composite deployable boom," *Composite Structures*, Vol. 113, 2014, pp. 429–436.

[12] Ferraro, S., and Pellegrino, S., "Self-deployable joints for ultra-light space structures," *2018 AIAA Spacecraft Structures Conference*, 2018, p. 0694.

[13] "Abaqus user manual," *Abaqus*, 2020.

[14] Luo, W., and Pellegrino, S., "Formation and propagation of buckles in coilable cylindrical thin shells with a thickness discontinuity," *International Journal of Solids and Structures*, Vol. 259, 2022, p. 112010.